JOURNAL OF CELLULAR PHYSIOLOGY 204:51–62 (2005)

Nestin-Expressing Neural Stem Cells Identified in the Scar Following Myocardial Infarction

JESSICA DRAPEAU,[1,2] VIVIANE EL-HELOU,[1,2] ROBERT CLEMENT,[1] SAMAR BEL-HADJ,[1,2] HUGUES GOSSELIN,[1] LOUIS-ERIC TRUDEAU,[3] LOUIS VILLENEUVE,[1] AND ANGELINO CALDERONE[1,2]*

[1]*Department of Physiology, University of Montreal, Montreal, Quebec, Canada*
[2]*Montreal Heart Institute, Montreal, Quebec, Canada*
[3]*Department of Pharmacology, University of Montreal, Montreal, Quebec, Canada*

Nerve fiber innervation of the scar following myocardial damage may have occurred either via the growth of pre-existing fibers and/or the mobilization of neural stem cells. The present study examined whether neural stem cells were recruited to the infarct region of the rat heart following coronary artery ligation. The neural stem cell marker nestin was detected in the infarct region of 1-week post-myocardial infarct (MI) male rats and cultured scar-derived neural-like cells. By contrast, nestin staining was undetected in either scar myofibroblasts or cardiac myocytes residing in the non-infarcted left ventricle. Reactive astrocytes were isolated from the infarct region and characterized by the co-expression of nestin, glial fibrillary acidic protein, and vimentin. Specific staining of oligodendrocytes and neurons was also detected in the infarct region and cultured scar-derived neural-like cells. Furthermore, neurofilament-M positive fibers were identified in the scar and tyrosine hydroxylase immunoreactivity was observed in peripherin-positive neurons. Neurite formation was induced in PC12 cells treated with the conditioned-media of primary passage scar-derived cells, highlighting the synthesis and secretion of neurotrophic factors. Nerve growth factor (NGF) and brain-derived neurotrophic factor were detected in myofibroblasts and neural cells, and both cell types expressed the NGF receptors trkA and p75. These data highlight the novel observation that neural stem cells were recruited to the infarct region of the damaged rat heart and may contribute in part to nerve fiber growth and subsequent innervation of the scar. J. Cell. Physiol. 204: 51–62, 2005.

Scar formation of the damaged heart following coronary artery ligation was defined as reparative fibrosis and constituted an essential physiological event that prevented cardiac rupture (Sun and Weber, 2000). The myofibroblast, characterized by the concomitant expression of α-smooth muscle actin and vimentin was the principal cell implicated in reparative fibrosis (Gabbiani, 1998). In response to local growth factors and inflammatory cytokines, myofibroblast proliferation was associated with the increased synthesis and deposition of extracellular matrix proteins that led to the formation of a collagen scar (Gabbiani, 1998). Concomitant with scar formation was the observation that Schwann cells and axons were detected along the periphery and within the damaged region of the heart induced by either coronary artery occlusion or transdiaphragmatic freeze-thaw injury (Vracko et al., 1990). The authors concluded that nerve fiber regeneration occurred in the newly formed scar of the damaged heart. A similar paradigm was described during cutaneous scar formation and healing as sensory nerve innervation and/or sprouting had occurred and was facilitated in part by the local release of nerve growth factor (NGF) by invading myofibroblasts (Matsuda et al., 1998; Liu et al., 1999; Hasan et al., 2000). Nerve fiber regeneration and subsequent innervation of the scar, regardless the tissue may have occurred either via the growth of pre-existing fibers and/or the recruitment of neural stem cells. Indirect evidence to support the latter premise was recently reported as multipotent stem cells were identified in the dermis and differentiated in culture to neural cells (Toma et al., 2001). The neural stem cell marker nestin was co-expressed with the neuron-specific markers βIII-tubulin and neurofilament-M (Lendahl et al., 1990; Toma et al., 2001). Moreover, nestin-positive neural stem cells in the dermis further differentiated to either an astrocyte or oligodendrocyte (Toma et al., 2001). In the CNS, the mobilization of resident stem cells represented a putative response to tissue damage, and the scar microenvironment provided the appropriate stimuli to induce nestin-expressing neural stem cell differentiation to neurons and/or astrocytes (Johansson et al., 1999; Rice et al., 2003).

Recent studies support the premise that the infarct region of the damaged heart was capable of recruiting stem cells. The injection of either Sca-1 positive cardiac progenitor cells or c-Kit positive bone marrow cells in the peri-infarct region of the heart were subsequently identified in the scar (Orlic et al., 2001; Oh et al., 2003). Based on these latter observations and the postulated role of neural stem cell recruitment to damaged tissue, the present study examined whether scar formation post-myocardial infarct (MI) mobilized nestin-expressing neural stem cells. Second, the differentiation of neural stem cells to either a neuron, astrocyte, and/or oligodendrocyte phenotype was examined. Lastly, as

Contract grant sponsor: Heart and Stroke Foundation of Canada; Contract grant sponsor: Quebec, Canadian Institutes of Health Research; Contract grant sponsor: "La Fondation de l'Institut de Cardiologie de Montréal."

*Correspondence to: Angelino Calderone, Research Center, Institut de Cardiologie de Montréal, 5000 rue Bélanger Est, Montréal, Québec, Canada H1T 1C8.
E-mail: angelo.calderone@umontreal.ca

Received 10 August 2004; Accepted 13 October 2004

DOI: 10.1002/jcp.20264

described during cutaneous wound healing, the potential synthesis of neurotrophic factors by scar myofibroblasts was elucidated.

METHODS

Myocardial infarct model, hemodynamics, and isolation of scar-derived cells

MI was induced in male Sprague–Dawley rats (9–11 weeks old; Charles Rivers, Canada) by ligating the left anterior descending coronary artery as previously described (Nguyen et al., 2003). In 1-week post-MI rats, left ventricular hemodynamics were measured by a microtip pressure transducer catheter (model SPR-407, 2F, Millar, Houston, TX), as previously described (Nguyen et al., 2003). The use and care of laboratory rats was according to the Canadian Council for Animal Care and approved by the Animal Care Committee of the Montreal Heart Institute. Following hemodynamic analysis, the infarct region was dissected from the non-infarcted left ventricle and placed immediately in chilled HBSS (Ca^{2+}-free; GIBCO, Burlington, Ontario). Pooled infarcts of variable size of 5–6 rats were digested with 0.1% trypsin (GIBCO) in HBSS overnight at 4°C. Scar-derived cells were subsequently recovered by repeated digestions in 10 ml of 0.1% collagenase (Type II; GIBCO). The supernatants collected from each digestion were centrifuged and re-suspended in a total volume of 30 ml in DMEM containing 7% heat-inactivated FBS (GIBCO). A 500 μl aliquot of the supernatant was added to P12 dishes containing glass coverslips and 6–7 ml added to T75 flasks. The media was changed 3–5 days following initial plating, and subsequently changed every 2 days until confluency was attained.

PC12 cells and treatment with supernatant of primary passage scar-derived cells

Pheochromocytoma cells (ATCC, Rockville, MD) were initially grown in T75 flasks containing F12K media supplemented with 15% horse serum, 2.5% FBS, and 1.5 g/L of sodium bicarbonate, and subsequently plated on glass coverslips coated with collagen type II (10 mg/100 ml). Conditioned-media (500 μl) was harvested from primary passage scar-derived cells 8–10 days following initial plating (two separate experiments of pooled infarcts of 1 week-post MI rats were examined) and applied twice to PC12 cells during a period of 5 days. FBS (7%) alone had no effect on neurite formation. The cells were fixed, phase contrast pictures were taken, and differentiation was examined via the reorganization of neurofilament-M (please see Immunofluorescence Protocol). In parallel experiments, either 50 ng/ml or 100 ng/ml of 2.5S NGF was applied twice to PC12 cells during a period of 5 days. The Adobe photoshop 6.0 program was used to measure the relative ratio of neurite/soma length of PC12 cells.

Western blot analysis of NGF and tyrosine hydroxylase

Scar-derived primary passage cells were grown to confluency in T75 flasks, and subsequently passaged with trypsin-EDTA (0.25%, 0.53 mM). First passage cells were plated at a density of 200 cells/mm^2 in DMEM containing 7% FBS for 36–48 h. The media was subsequently changed to serum-free and cells harvested 2 days later. Cell lysates (100 μg) were collected from four separate experiments and prepared for detection of NGF by Western blot analysis, as previously described (Colombo et al., 2003). In parallel, 1st passage fibroblasts lysates obtained from the normal and non-infarcted left ventricle were probed for NGF expression. Fibroblasts were isolated as described above for scar myofibroblasts ($n = 2–3$). Tyrosine hydroxylase protein expression was examined in the infarct region of 1-week post-MI rats ($n = 3$). Isolated infarcts were homogenized in lysis buffer, and 100 μg protein lysates were used for Western blot analysis, as previously described (Nguyen et al., 2003). The antibodies employed include the rabbit polyclonal antibody (1:500) directed against NGF-β (Chemicon, Temecula, CA) and the mouse monoclonal antibody (1:500) directed against tyrosine hydroxylase (Chemicon). Following overnight incubation at 4°C, the appropriate secondary antibody-conjugated to horseradish peroxidase (1:10,000) was added, and visualization of the bands were detected by autoradiography utilizing the ECL detection kit (Amersham, Baie d'Urfe, Quebec).

ELISA measurements of NGF

Biologically active NGF was examined by an ELISA method (Chemicon) in the conditioned-media harvested from scar-derived cells (1 week post-MI rats). Four days following initial plating the cells were washed, and 500 μl of DMEM containing FBS was added, and denoted as day 0. The media was harvested from day 2 to 7. Each time point was examined in 3–4 separate experiments of pooled infarcts of variable size, and NGF was not detected in 7% FBS.

Polymerase chain reaction

RT-PCR was performed by standard methodology on total RNA isolated from the infarct region of 1-week post-MI rats and primary passage scar fibroblasts, as previously described (Nguyen et al., 2003). Two distinct sets of DNA primers were employed to detect the tyrosine hydroxylase transcript (Set 1; Forward, 5′-CGCTGAAGGGCCTCTATGCTAC-3′, and Reverse, 5′-GCATGGCGGATATACTGGGTG-3′, PCR product of 238 base pairs) (Set 2; Forward, 5′-GGTATATGTCACGCTGAAGGG-3′, and Reverse, 5′-CCGGCTCAGGTGAATGCATAG-3′, PCR product of 278 base pairs). The cycling profiles were 45 sec of denaturing (94°C), 30 sec of annealing (55°C), and 90 sec of extension (72°C) for 35 cycles, followed by a final extension step (10 min at 72°C). PCR products were separated by base pair size on gels using standard procedures. A non-specific band of 325–350 base pairs was also detected (data not shown). As a negative control, total RNA isolated from neonatal rat ventricular myocytes was employed.

Immunofluorescence staining of tissue and cells

The infarcted rat heart was excised and immersed directly in 2-methyl butane (temperature maintained at −80°C), and subsequently stored at −80°C. Immunofluorescence experiments were performed on cryocuts of 14 μm thickness from the hearts of 1-week post-MI rats ($n = 3$ rats for each protein examined). Primary passage scar-derived cells were plated on glass coverslips, and examined 5–10 days following initial plating. The myofibroblast phenotype was determined at 1–5 days following initial plating and concomitantly with neural specific proteins. Immunofluorescence detection of each protein was examined in 3–8 separate experiments consisting of 5–6 pooled infarcts of variable size from 1-week post-MI rats. Plated cells or cryocuts were fixed for 10–15 min in PBS (pH 7.4) containing-paraformaldehyde (4%), and subsequently incubated for 10–15 min with 50 mM NH_4Cl. Fixed cells or tissue were permeabilized with 0.2% triton X-100 in PBS-containing 2% BSA for 1–2 h at room temperature, and subsequently incubated overnight at 4°C with the appropriate antibody diluted in 0.05% triton X-100 in PBS-containing 2% BSA. Antibodies employed were the mouse monoclonal anti-vimentin (1:200; Sigma, St. Louis, MO), mouse monoclonal anti-α-smooth muscle actin (1:250; Sigma), mouse monoclonal anti-nestin (1:400; Clone rat-401; Chemicon), mouse monoclonal anti-myelin specific oligodendrocyte protein (1:400; Chemicon), mouse monoclonal anti-tyrosine hydroxylase (1:500; Chemicon), rabbit polyclonal anti-glial fibrillary acidic protein (1:1000; Chemicon), rabbit polyclonal anti-neurofilament-M (1:1000; Chemicon), rabbit polyclonal anti-peripherin (1:500-1000; Chemicon), rabbit polyclonal anti-NGF-β (1:300; Chemicon), rabbit polyclonal anti-trkA (1:1000; BD PharMingen, Oakville, Ontario), rabbit polyclonal anti-p75 (1:300; Chemicon), and rabbit polyclonal anti-brain-derived neurotrophic factor (1:500; Chemicon). Following incubation, cells were incubated for 1–2 h at room temperature with either goat anti-mouse IgG conjugated to rhodamine (1:250-500; Molecular Probes, Eugene, OR) or goat anti-rabbit IgG conjugated to fluorescein isothiocyanate (1:500; Jackson Laboratories, West Grove, PA) diluted in 0.05% triton X-100 in PBS-containing 2% BSA. Thereafter, fixed cells or tissue were washed with PBS, the coverslips mounted on DABCO medium (0.2 μM; Sigma), and observed with either a 10×- or 63×-oil 1.4 NA DIC plan apochromat objective mounted on a Zeiss Axiovert 100M

confocal microscope. A fluorescence signal was not detected when either fixed cells or tissue were incubated with either conjugated secondary antibody alone. An additional negative control experiment was performed as scar-derived cells were treated with normal serum containing rabbit IgG at a concentration of 11.9 μg/ml (corresponds to the highest concentration of rabbit polyclonal antibody employed in the study). As a positive control for neurofilament-M staining, mesencephalic neurons were isolated from the adult rat, as previously described (Gelais et al., 2004). Lastly, nuclear staining was performed with propidium iodide (Calbiochem, La Jolla, CA). Fixed cells (permeabilized with 0.2% triton X-100 in PBS-containing 2% BSA for 1–2 h at room temperature) were washed with SSC (2×), and subsequently treated with RNase (0.35 mg/ml) for 25 min at 37°C. Thereafter, cells were treated 20 min at room temperature with propidium iodide (5 μM in 2× SSC; Calbiochem), and staining visualized as described above ($n = 2$).

RESULTS

Neural-like cells expressing the stem cell marker nestin isolated in scar-derived primary passage cells and detected in the infarct region

In a subset of rats that underwent coronary artery ligation, the loss of ventricular tissue significantly decreased left ventricular systolic pressure, the rate of contraction (+dP/dt) and relaxation (−dP/dt) (Table 1). Following hemodynamic analysis, the infarct region of 1-week post-MI rats was removed, digested, and the isolated cells cultured in DMEM containing 7% FBS. One to two days following initial plating, α-smooth muscle actin and vimentin staining was detected in scar myofibroblasts, but were unorganized. By 3–5 days, α-smooth muscle actin and vimentin filaments were observed in scar myofibroblasts (Fig. 1C,D).

Interspersed among the myofibroblasts were cells with a neural-like morphology, characterized by a refractive cell body with one or more processes. After 4–7 days in culture, the processes increased in length and contact between neural-like cells was evident (Fig. 1A). By 10–14 days, the number of neural-like cells increased, and aggregates and/or clusters were seen (Fig. 1B). Numerous neural-like cells isolated from the scar region expressed the neural stem cell marker nestin (Lendahl et al., 1990), and staining was observed in the cell body and processes (Fig. 1E). By contrast, nestin immunoreactivity was not detected in surrounding fibroblasts, as visualized by propidium iodide staining of the nucleus (Fig. 1E). Consistent with these data, nestin-positive cells were identified in the infarct region of 1-week post-MI rats. Furthermore, in the peri-infarct region of the damaged heart, nestin immunoreactivity was observed in the non-infarcted zone of the left ventricle (Fig. 2). In a remote region of the non-infarcted left ventricle, nestin staining was not detected in cardiac myocytes (Fig. 2).

Reactive astrocytes, oligodendrocytes, and neurons detected in the infarct region and scar-derived primary passage cells

During development, immature astrocytes expressed nestin and vimentin, whereas both proteins were replaced by the intermediate filament glial fibrillary acidic protein (GFAP) following maturation (Lin et al., 1995; Menet et al., 2001). Tissue damage and subsequent scar formation in the CNS was associated with the recruitment of GFAP-expressing astrocytes that re-expressed both vimentin and nestin, and were redefined as reactive astrocytes (Lin et al., 1995; Menet et al., 2001). In a subpopulation of nestin-expressing neural cells isolated from the scar, GFAP immunoreactivity was detected in the cytoplasm and processes, whereas a weak nuclear signal was observed in a limited number of cells (Fig. 3). Moreover, GFAP-containing astrocytes expressed vimentin (Fig. 3). Collectively, these data support the premise that reactive astrocytes resided in the infarct region. Nestin-expressing neural stem cells were also described as progenitor cells of oligodendrocytes (Almazan et al., 2001). Indeed, myelin oligodendrocyte specific protein (MOSP) immunoreactivity was detected in a subpopulation of neural cells in vitro and the infarct region (Figs. 3 and 4). Lastly, in the skin and following brain damage, nestin-expressing neural stem cells differentiated to a neuronal phenotype (Toma et al., 2001; Rice et al., 2003). In the infarct region, peripherin- and neurofilament-M-positive cells were identified and myelin oligodendrocyte-specific protein immunoreactivity was absent (Fig. 4). Moreover, fibers were detected in the scar region and stained positive for peripherin and neurofilament-M (Fig. 4). As a positive control, numerous neurofilament-M-positive axons were detected emanating from a rat mesencephalic neuron (Fig. 4). Consistent with the in vivo data, peripherin and neurofilament-M immunoreactivity were detected in scar-derived neural-like cells (Fig. 5). In cultured primary passage scar-derived cells, nestin and neurofilament-M co-expression was detected supporting a progenitor role of nestin-expressing neural stem cells. In some cells, nestin expression was associated with a weak level of neurofilament-M immunoreactivity (Fig. 5). A transitional phase of differentiation was apparent as the immunoreactive signal of neurofilament-M was detected in a diffused pattern in the cytoplasm, whereas nestin expression was partially filamentous (Fig. 5). Lastly, neurons expressing predominantly neurofilament-M and a weak level of nestin immunoreactivity were identified (Fig. 5). Consistent with this latter observation, nestin immunoreactivity was not co-localized with neurofilament-M positive fibers in the infarct region (Fig. 4). To further delineate the phenotype, the expression of the sympathetic neuronal protein tyrosine hydroxylase was examined. In total RNA isolated from the infarct region of 1-week post-MI rats and primary passage scar-derived cells, tyrosine hydroxylase mRNA was expressed, whereas the transcript was undetectable in neonatal rat ventricular myocytes (Fig. 6). Consistent with these data, tyrosine hydroxylase protein (~59–61 kDa) was detected in the infarct region of 1-week post-MI rats ($n = 3$) (Fig. 6). Lastly, in scar-derived peripherin-positive neural cells, tyrosine hydroxylase immunoreactivity was granular in appearance in the cytoplasm, and in some cells concomitant with an intense perinuclear signal (Fig. 6). Moreover, granular staining of tyrosine hydroxylase was also detected in the nucleus (Fig. 6).

Treatment of PC12 cells with conditioned media of scar-derived primary passaged cells induced neurite formation

The presence of neuronal cells in the infarct region of the heart supported the premise that neurotrophic factors were synthesized and secreted by scar-derived cells. Pheochromocytoma (PC12) cells treated for 5 days with 7% FBS did not exhibit any detectable evidence of neurite formation. By contrast, newly formed neurites (neurite/soma length ratio = 4.8 ± 0.54; $n = 188$ cells examined) were evident following a 5-day exposure of PC12 cells to the conditioned-media harvested from scar-derived primary passage cells (Fig. 7).

TABLE 1. Heart weight and contractile function of the myocardial infarct (MI) rat

	BW (g)	HW (g)	Scar (g)	LVSP (mmHg)	LVEDP (mmHg)	LV +dP/dt (mmHg/sec)	LV −dP/dt (mmHg/sec)
Sham ($n = 9$)	324 ± 14	1.04 ± 0.12	—	141 ± 9	14 ± 3	6275 ± 320	4702 ± 300
MI ($n = 9$)	309 ± 5	1.18 ± 0.05	$0.04 \pm 0.0.01$[a]	112 ± 5[a]	14 ± 3	5323 ± 175[a]	3730 ± 100[a]

BW, body weight; HW, heart weight; LVSP, left ventricular systolic pressure; LVEDP, left ventricular end-diastolic pressure; +dP/dt, rate of contraction; −dP/dt, rate of relaxation; data are presented as mean ± S.E.M.; [a] represents $P < 0.05$ versus Sham; and n number of rats.

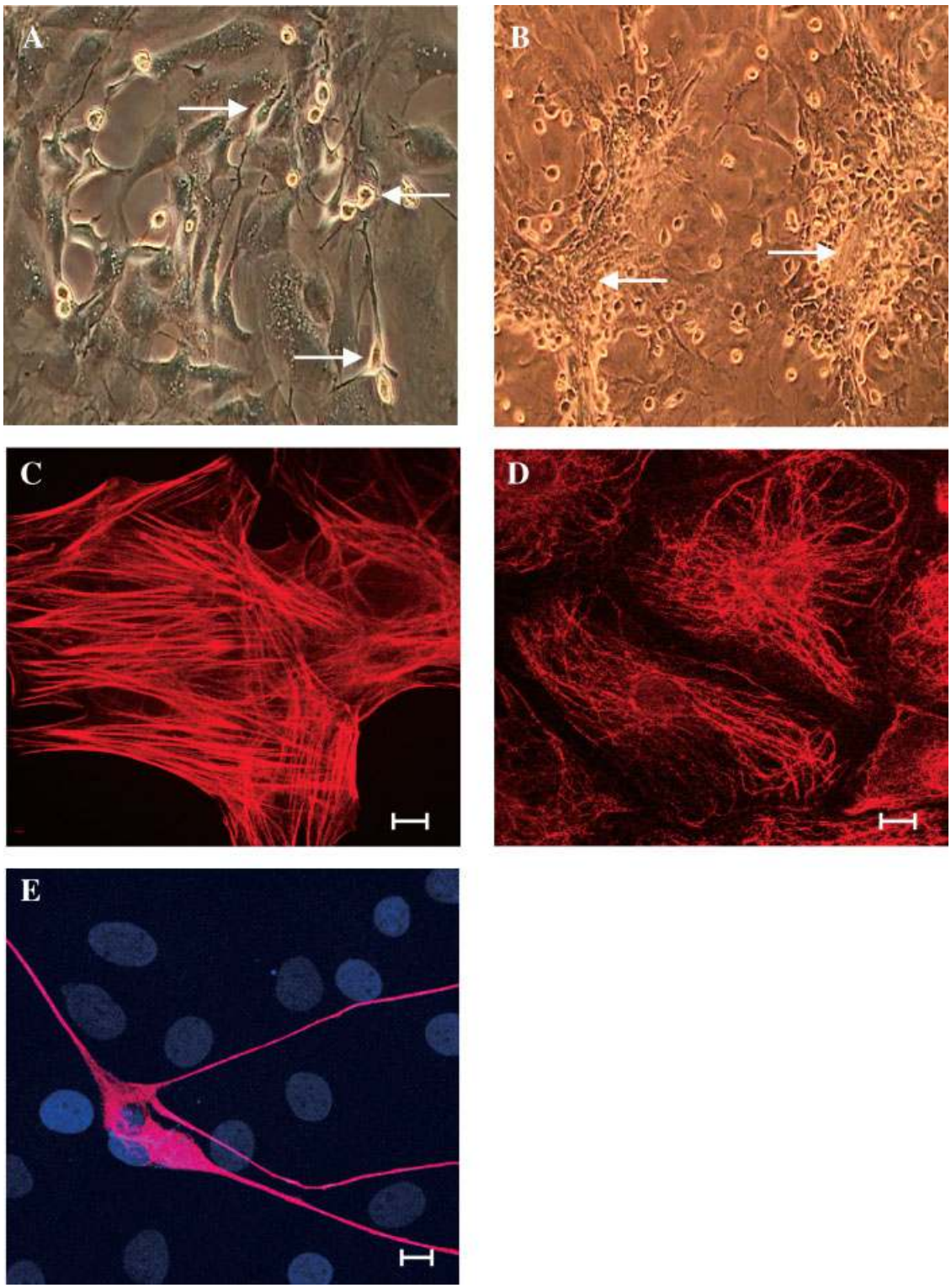

Fig. 1. Nestin-expressing neural stem cells and myofibroblasts detected in scar-derived primary passage cells. **Part A**: Neural-like cells (several cells indicated by arrow) with processes and contacts between neighboring cells were observed 4–7 days following initial plating (20× magnification). **Part B**: Aggregates of neural-like cells (indicated by arrow) 10–14 days following initial plating were observed (10× magnification). Myofibroblasts expressed α-smooth muscle actin (**part C**) and vimentin (**part D**). **Part E**: A nestin-positive neural cell was detected in scar-derived primary passage cells. By contrast, nestin immunoreactivity was not observed in surrounding myofibroblasts, as visualized by propidium iodide staining of the nucleus. Scale bar, 10 μm.

PC12 cell differentiation was further delineated by the reorganization of neurofilament-M in the cytoplasm and neurites (Fig. 7). As a positive control, PC12 cells were treated with NGF for a period of 5 days and neurite formation was detected with either 50 ng/ml (neurite/soma length ratio $= 6.03 \pm 0.68$; $n = 30$ cells) or 100 ng/ml (neurite/soma length ratio $= 5.86 \pm 0.37$; $n = 51$ cells examined) of the peptide. Neurite formation was comparable between the conditioned media of scar-derived primary passage cells and exogenous NGF. These data demonstrate that glial cells, neurons, and/or possibly myofibroblasts synthesized and secreted neurotrophic factors. Furthermore, the local release of neurotrophic factors may

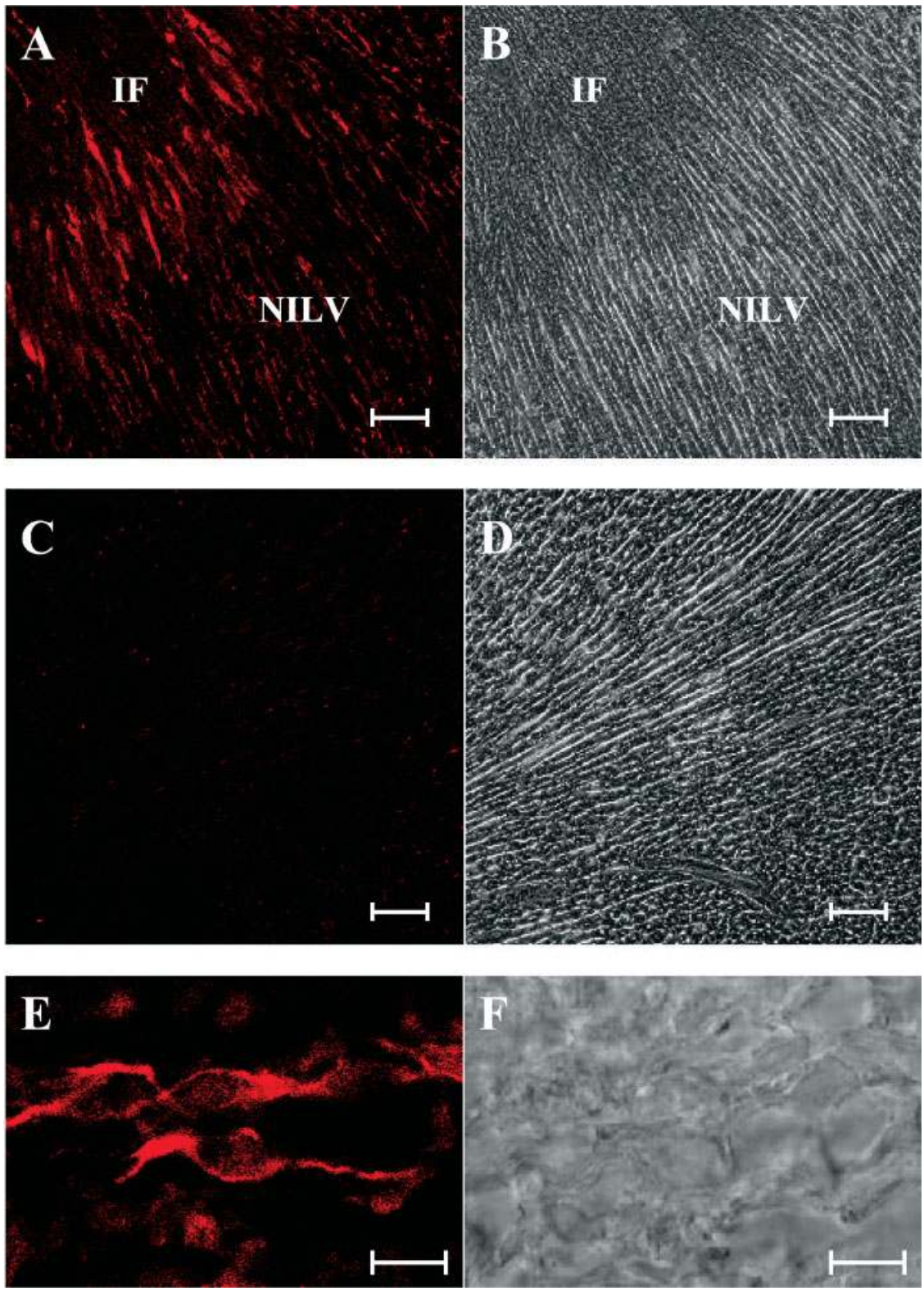

Fig. 2. Nestin immunoreactivity was detected in the infarct and non-infarcted regions of the rat heart. **Part A**: Nestin staining was detected in the infarct (IF) and non-infarcted left ventricle (NILV) residing at the peri-infarct zone. **Part B**: Phase contrast picture of part (A). **Part C**: Nestin staining was not detected in a remote region of the non-infarcted left ventricle. **Part D**: Phase contrast picture of part (C). **Part E**: Nestin-expressing neural stem cells were identified in the infarct region, whereas immunoreactivity was not detected in scar myofibroblasts (please see Fig. 1). **Part F**: Phase contrast picture of part (E). Parts (A–D): Scale bar, 100 μm; parts (E & F): Scale bar, 10 μm.

facilitate the secondary expression of neuronal-specific proteins in scar myofibroblasts. A variable nuclear and cytoplasmic signal of neurofilament-M was detected in myofibroblasts. Moreover, although modest in number, neurofilament-M filaments were observed in myofibroblasts (Fig. 7). Unexpectedly, GFAP expression was also detected in the nucleus of myofibroblasts accompanied by a variable cytoplasmic signal and organized filaments in a minority of cells (Fig. 7). The variable nuclear signal of GFAP and neurofilament-M in myofibroblasts were indeed specific as staining was undetected

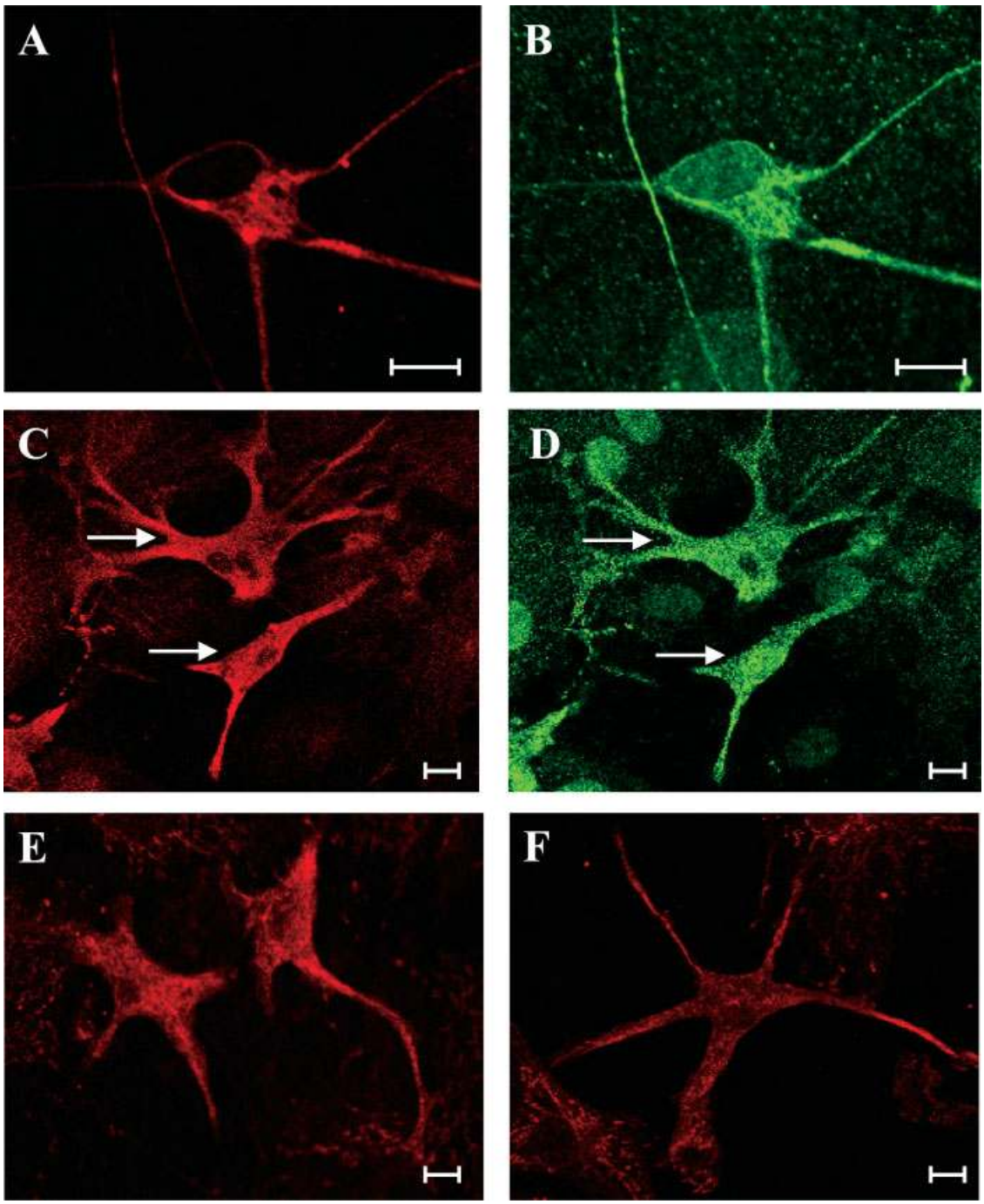

Fig. 3. Reactive astrocytes and oligodendrocytes detected in scar-derived primary passage cells. The co-expression of nestin (**part A**) and glial fibrillary acidic protein (**part B**). The co-expression of vimentin (**part C**) and glial fibrillary acidic protein (**part D**). **Parts E** & **F**: Oligodendrocytes expressing myelin specific oligodendrocyte protein. Arrows indicate cells examined. Scale bar, 10 μm.

following the treatment with normal serum containing rabbit IgG (Fig. 7). Lastly, in NIH 3T3 fibroblasts, neither GFAP nor neurofilament-M staining was observed (data not shown).

Nerve growth factor, brain-derived neurotrophic factor, trkA, and p75 detected in scar-derived cells

The neurotrophins NGF and brain-derived neurotrophic factor (BDNF) were synthesized in glial cells and neurons and implicated in neuronal cell differentiation and survival (Gunn-Moore and Tavaré, 1998; Hee Han and Holtzman, 2000). Moreover, during cutaneous wound healing, NGF expression was detected in invading myofibroblasts (Matsuda et al., 1998; Liu et al., 1999). Utilizing an ELISA method, biologically active NGF was detected in the media of primary passage scar-derived cells and the temporal increase may in part reflect increased cell proliferation and/or synthesis (Fig. 8). Western blot analysis of 1st passage scar myofibroblasts revealed several immunoreactive bands of NGF at ~27 and ~19 kDa that corresponded to long and short forms of unprocessed NGF (Edwards et al., 1988; Fahnestock, 1991; Delsite and Djakiew, 1999) (Fig. 8). Moreover, the level of unprocessed NGF in scar-derived myofibroblasts was comparable to that observed in 1st passage fibroblasts isolated from the normal and non-infarcted left ventricle (Fig. 8). In two separate experiments, a ~13 kDa band was detected (data not shown) and corresponded to the

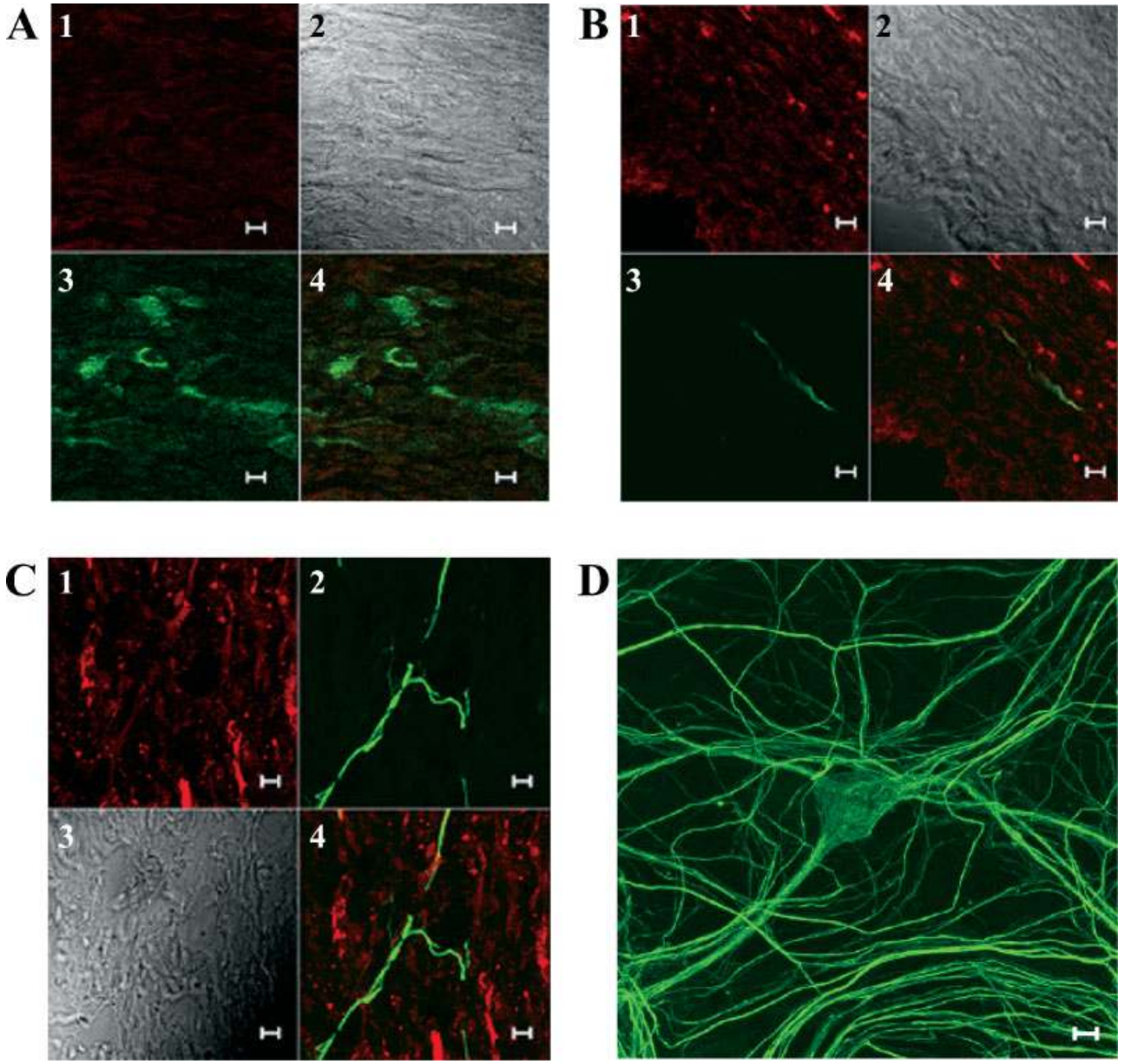

Fig. 4. Neurofilament-M, peripherin, myelin oligodendrocyte specific protein (MOSP) and nestin immunoreactivity detected in the infarct region. **Part A**: MOSP (Fig. 1) staining did not co-localize with peripherin-positive cells (Figs. 3 and 4). Phase contrast picture of the scar (Fig. 2). **Part B**: MOSP (Fig. 1) staining was detected in the infarct region and did not co-localize with a peripherin-positive fiber (Figs. 3 and 4). Phase contrast picture of the scar (Fig. 2). **Part C**: Nestin (Fig. 1) immunoreactivity was detected in the infarct region and did not co-localize with a neurofilament-M positive fiber (Figs. 2 and 4). Phase contrast picture of the scar (Fig. 3). **Part D**: Neurofilament-M staining of processes emanating from a rat mesencephalic neuron (photo is a maximum projection of a z-stack). Scale bar, 10 μm.

biologically active NGF protein (Fahnestock, 1991). Collectively, these data suggest that NGF expression represented a conserved phenotype of fibroblasts residing in the myocardium. Immunofluorescence experiments confirmed the Western blot data, as NGF immunoreactivity was consistently observed in the cytoplasm and nucleus of α-smooth muscle actin-positive myofibroblasts, however, the intensity was variable (Fig. 9). Moreover, in some but not all myofibroblasts, NGF staining was detected on actin filaments (Fig. 9). NGF released from myofibroblasts may act in an autocrine fashion as the cognate high-affinity receptor trkA and low-affinity receptor p75 were detected in the cytoplasm, on the plasma membrane, and co-incident with an intense nuclear signal in a majority of the cells examined (Fig. 9). NGF was likewise detected in neural cells, as immunoreactivity was localized in the perinuclear/nuclear region and on filaments located in the processes (Fig. 9). An intense granular cytoplasmic NGF signal was also observed, and the disparate patterns of expression may in part be dependent of the neural cell phenotype. Furthermore, neural cells expressed trkA, as a granular signal was observed in the cytoplasm and nucleus, and detected on the plasma membrane (Fig. 9). Akin to trkA, a granular cytoplasmic signal of p75 was observed in neural cells, and a modest number of cells were associated with a nuclear signal. Lastly, α-smooth muscle actin negative neural cells expressed BDNF, as an intense granular cytoplasmic signal was detected, whereas nuclear staining was observed in a limited number of cells (Fig. 9). Surprisingly, a modest immunoreactive BDNF signal was detected in the perinuclear/nuclear region of scar myofibroblasts (Fig. 9).

DISCUSSION

Only recently has the infarct region of the heart been considered a dynamic tissue (Sun and Weber, 2000). Scar formation required the interplay of inflammatory cytokines

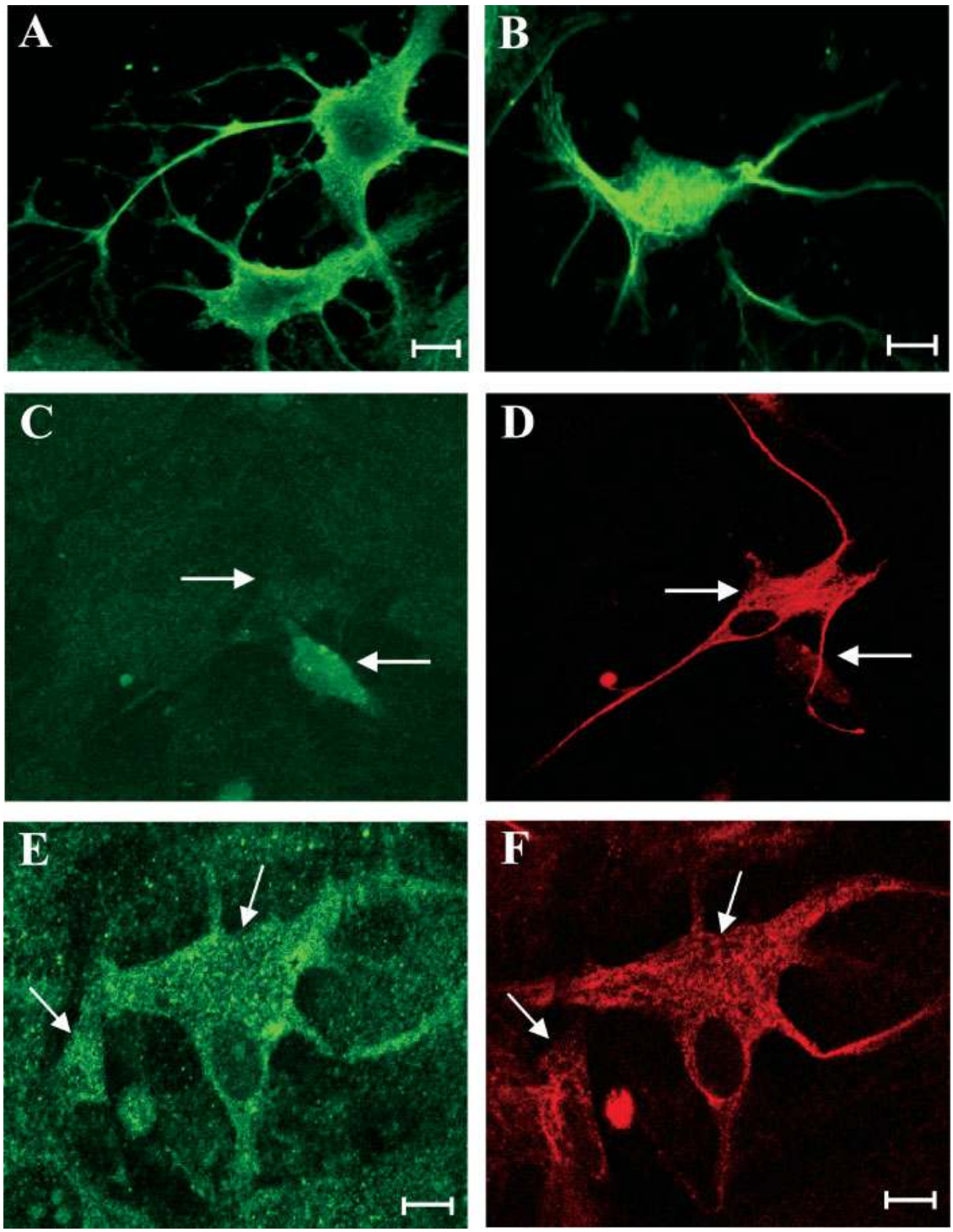

Fig. 5. Neurofilament-M- and peripherin-positive neural cells detected in scar-derived primary passage cells. Neurofilament-M- (**part A**) and peripherin-positive (**part B**) neurons. Two cells identified with a disparate pattern of neurofilament-M (**part C**) and nestin expression (**part D**). In two distinct cells, neurofilament-M immunoreactivity (**part E**) was diffused and co-expressed partially organized nestin filaments (**part F**). Arrows indicate cells examined. Scale bar, 10 μm.

transforming fibroblasts to myofibroblasts, their subsequent recruitment to the site of damage, proliferation, and subsequent deposition of extracellular matrix proteins (Gabbiani, 1998; Sun and Weber, 2000). Concomitant with scar formation was the observation that Schwann cells and axons were detected along the periphery and within the damaged region of the heart (Vracko et al., 1990). These observations were recently reaffirmed as neuronal fibers were detected in the infarct region of the damaged dog heart (Zhou et al., 2004). However, it remains unknown as to whether nerve fiber innervation of the scar proceeded either by the growth or pre-existing fibers and/or the recruitment of neural stem cells. The present study has demonstrated that scar formation in the heart following left anterior coronary artery occlusion in the adult male rat recruited neural stem cells expressing the intermediate filament protein nestin. Indirect in vitro evidence supported the premise that nestin-expressing neural stem cells may have differentiated to reactive astrocytes, neurons,

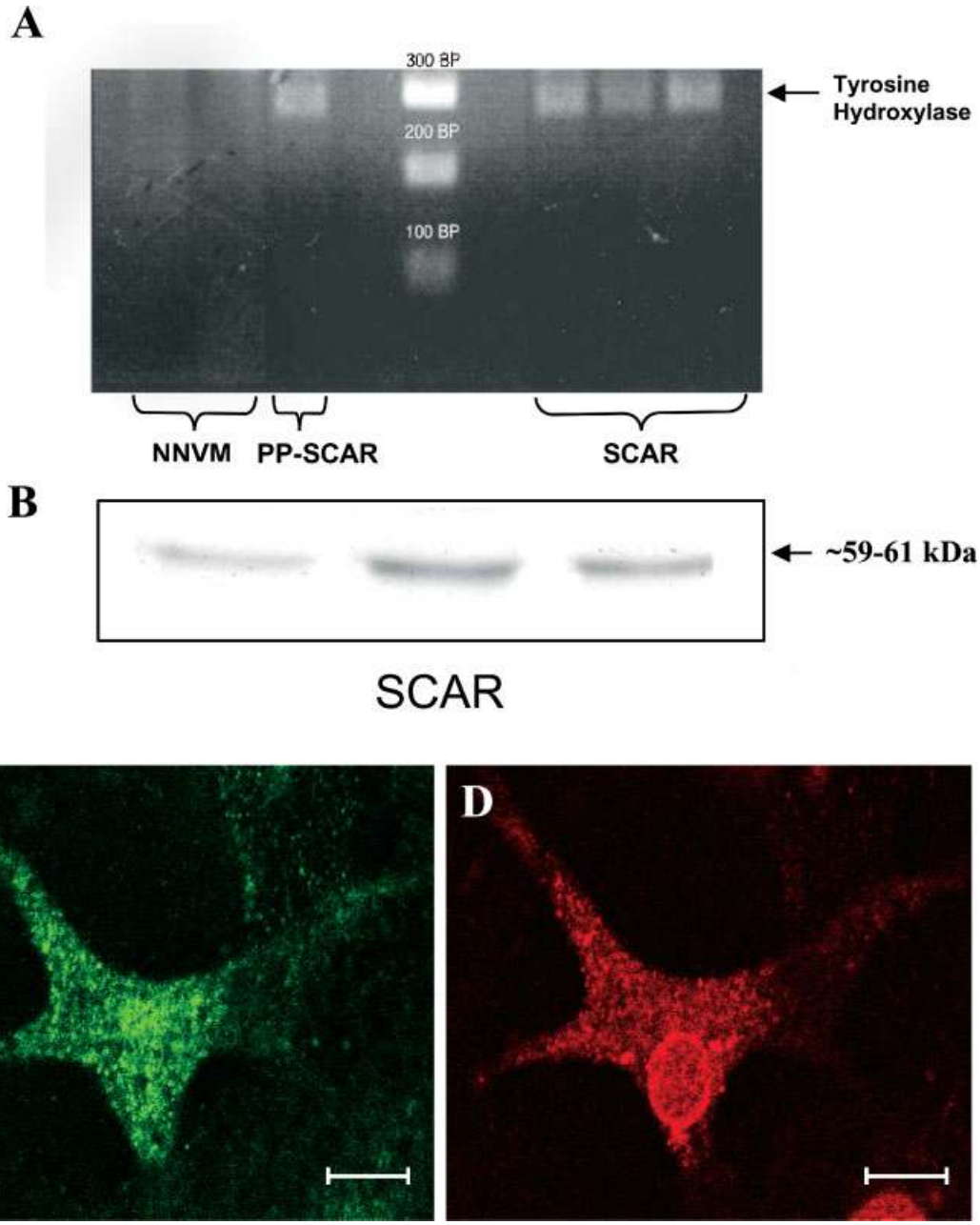

Fig. 6. Tyrosine hydroxylase mRNA and protein expression. **Part A**: PCR product of 278 base pairs corresponding to a specific region of the tyrosine hydroxylase transcript was observed in total RNA isolated from the scar of 1-week post-MI rats, and primary passage scar-derived cells (PP-SCAR). A signal was not observed in neonatal rat ventricular myocytes (NNVM). **Part B**: Tyrosine hydroxylase protein (~59–61 kDa) was detected in the infarct region of 1-week post-MI rats ($n = 3$). A peripherin- (**part C**) and tyrosine hydroxylase-positive (**part D**) neuron. Scale bar, 10 μm.

and oligodendrocytes. Moreover, neuronal innervation of the infarct region had apparently occurred as peripherin- and neurofilament-M positive fibers were detected. The local synthesis of NGF and BDNF by scar myofibroblasts and neural cells may have in part facilitated the differentiation of neural stem cells to a neuronal phenotype and subsequent innervation.

In the developing CNS, expression of the intermediate filament protein nestin was defined as a putative phenotypic marker of multipotent neural stem cells (Lendahl et al., 1990; Johansson et al., 1999). Studies have demonstrated that during neurogenesis, nestin was replaced by the intermediate neurofilaments (Lendahl et al., 1990). Likewise, the loss of nestin expression during astrocyte maturation was associated with the concomitant induction of the intermediate filament protein glial fibrillary acidic protein (Lendahl et al., 1990). However, following brain injury, the re-expression of nestin and vimentin were detected in mature astrocytes and redefined as reactive astrocytes (Lin et al., 1995; Menet et al., 2001). Lastly, nestin expression was characterized as a marker of proliferating pre-oligodendrocytes and subsequently down-regulated in post-mitotic mature oligodendrocytes (Almazan et al., 2001). A similar paradigm was demonstrated in the mammalian dermis, as nestin-expressing neural stem cells isolated from the skin differentiated either to a neuron, astrocyte, or oligodendrocyte (Toma et al., 2001). In the present study, nestin-positive cells were detected in the infarct region of the damaged rat heart. Consistent with these data, neural cells isolated from the scar of post-MI rats expressed the intermediate filament protein nestin, whereas immunoreactivity was absent in myofibroblasts. Moreover, nestin immunoreactivity was also detected in the non-infarcted zone of the

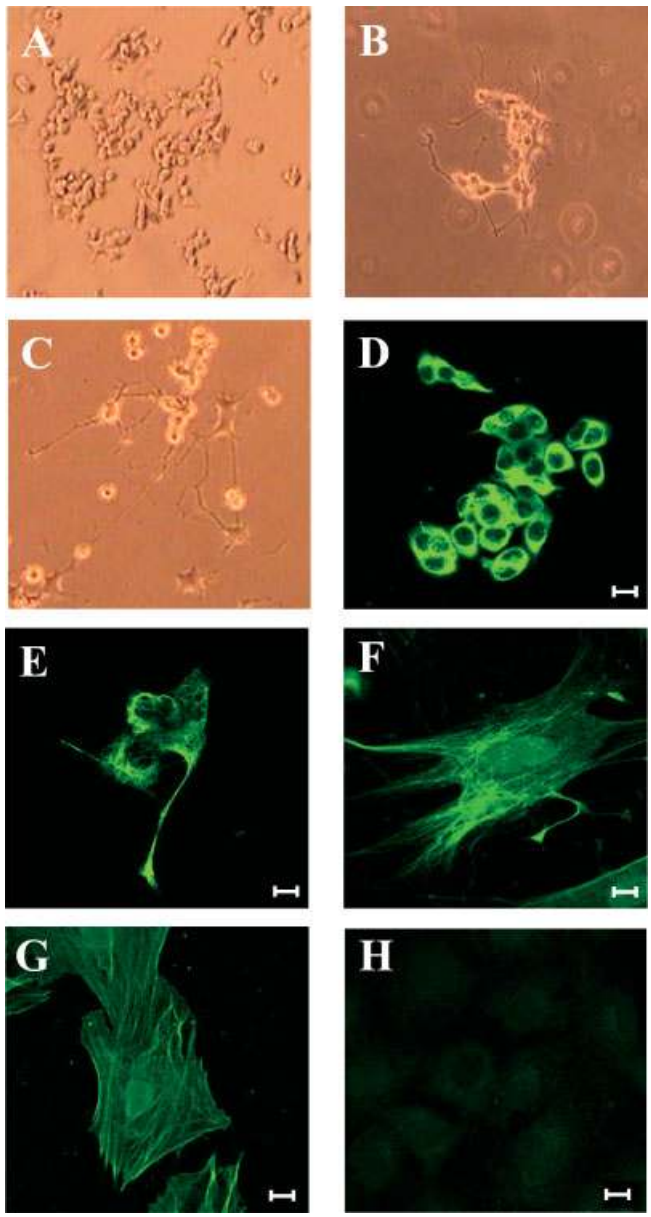

Fig. 7. PC12 cell differentiation and neural protein expression in myofibroblasts. **Part A**: Phase contrast picture of undifferentiated PC12 cells (20× magnification). PC12 differentiation following the treatment with the supernatant harvested from scar-derived cells (**part B**) or 50 ng/ml of nerve growth factor (NGF) (**part C**) (20× magnification). **Part D**: Neurofilament-M expression was diffused and unorganized in undifferentiated PC12 cells. **Part E**: Neurofilament-M filaments were detected in PC12 cells following the treatment with the supernatant harvested from scar-derived cells. Myofibroblasts expressed neurofilament-M (**part F**) and glial fibrillary acidic protein (**part G**) in the nucleus and in some cells, organized filaments were apparent. **Part H**: Normal serum rabbit IgG signal in scar myofibroblasts. Scale bar, 10 μm.

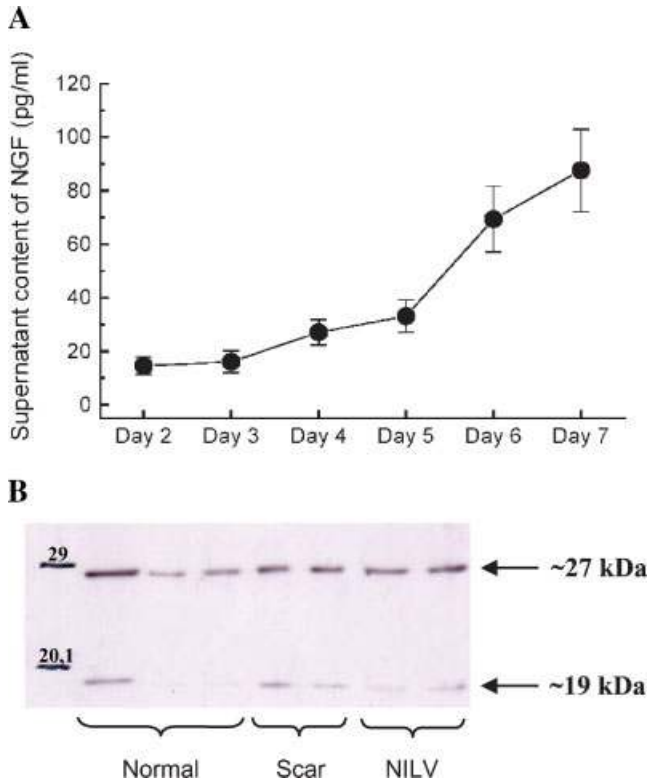

Fig. 8. NGF synthesized and secreted by scar-derived primary passage cells. **Part A**: Utilizing an ELISA method, biologically active NGF was detected in the supernatant of primary passage scar-derived cells. **Part B**: Western blot analysis of unprocessed NGF in 1st passage scar-derived myofibroblasts, normal and non-infarcted left ventricular fibroblasts.

peri-infarct region. It is tempting to speculate that the nestin-positive cells detected in the latter region may represent neural stem cells migrating to the infarct site. By contrast, nestin immunoreactivity was not detected in cardiac myocytes residing in a remote region of the non-infarcted left ventricle. Collectively, these data support the premise that neural stem cells were recruited to the damaged region of the heart. The source and phenotype of the progenitor cell that gave rise to nestin-expressing neural stem cells in the scar region remains presently undefined. As demonstrated in the mammalian dermis, the normal heart may contain multipotent stem cells (Toma et al., 2001) and following damage differentiated to a neural stem cell phenotype. Alternatively, either bone marrow hematopoietic or mesenchymal stem cells may have migrated to the infarct site, as both cell types were shown to differentiate to a neural progenitor cell in vitro under the appropriate conditions (Sanchez-Ramos et al., 2000; Hao et al., 2003).

In the damaged myocardium, innervating axons in the scar were complexed with Schwann cells that had extensive branched processes (Vracko et al., 1990). Schwann cells have been characterized as oligodendrocytes of the peripheral nervous system (Rogister et al., 1999). In the present study, a subpopulation of neural cells identified in the infarct region and isolated from the scar expressed myelin specific oligodendrocyte protein, supporting the differentiation of oligodendrocytes/Schwann cells. Although not examined, it is our contention that nestin-expressing neural stem cells gave rise to oligodendrocytes. Indeed, previous studies have confirmed this latter thesis (Almazan et al., 2001), and in vitro data from the present study indirectly supported the premise that nestin-expressing neural stem cells further differentiated to reactive astrocytes and neurons. Moreover, peripherin- and neurofilament-M positive fibers were identified in the infarct region of 1 week post-MI rats. These data were consistent with two previous studies demonstrating the presence of innervating axons in the damaged region of the heart (Vracko et al., 1990; Zhou et al., 2004). Moreover, in the infarct region of the damaged dog heart, tyrosine hyxroxylase mRNA and protein were identified (Zhou et al., 2004). Consistent with these latter observations, tyrosine hydroxylase protein and mRNA were detected in the infarct site, and immunoreactivity observed in peripherin-positive neural cells. Collectively, these data suggest that the scar microenvironment of the damaged rat heart expressed the appropriate stimuli to facilitate the differentiation of oligodendrocytes/Schwann cells, reactive astrocytes, and neurons with a sympathetic phenotype.

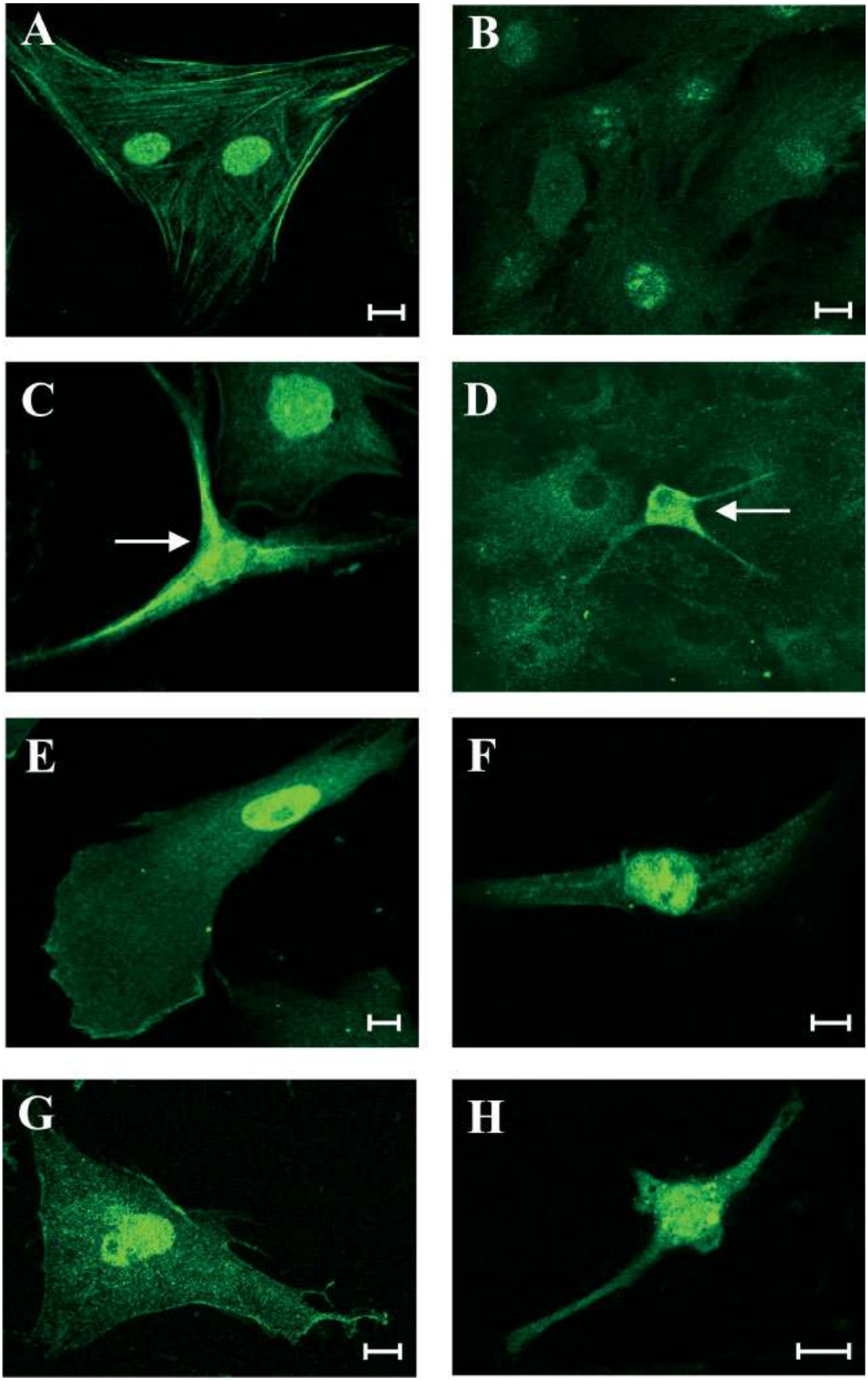

Fig. 9. NGF, brain-derived neurotrophic factor (BDNF), trkA and p75 expression in scar-derived primary passage cells. **Parts A** and **B**: NGF expression in myofibroblasts was detected in the cytoplasm, and nucleus. In some myofibroblasts, NGF staining was also detected on actin filaments, albeit the intensity was variable. **Part C**: In numerous neural-like cells, NGF immunoreactivity was observed in the nuclear/perinuclear regions and located on filaments within the processes (indicated by arrow). **Part D**: A granular cytoplasmic signal of BDNF was detected in a neural cell (indicated by arrow) whereas a modest perinuclear signal was observed in myofibroblasts. TrkA and p75 receptors were detected in the nucleus and plasma membrane of myofibroblasts (**parts E** & **G**) and neural cells (**parts F** & **H**). Scale bar, 10 μm.

Neuronal innervation of the infarct region and the isolation of scar-derived neurofilament-M and peripherin-positive neurons have provided the impetus to examine whether scar-derived cells synthesized and secreted neurotrophic factors. Indeed, the treatment of PC12 cells with the conditioned-media harvested from primary passage scar-derived cells induced neurite formation and the reorganization of neurofilament-M. During cutaneous wound healing, it has been postulated that sensory nerve innervation and/or sprouting was mediated by the release of NGF by invading myofibroblasts (Matsuda et al., 1998; Liu et al., 1999; Hasan et al., 2000). Based on this observation, the present study examined the potential synthesis of the neurotrophic factor NGF by scar-derived cells. Biologically active NGF was detected in the media of primary passage scar-derived cells. Western blot analysis confirmed NGF synthesis by scar-derived cells, and immunoflourescence experiments revealed that the neurotrophic factor was detected in the cytoplasm and the perinuclear/nuclear region of both scar myofibroblasts and neural cells. Co-incident with nuclear NGF staining, trkA and p75 receptors were localized in the nucleus and detected on the plasma membrane. A nuclear signal of either NGF or its cognate receptors was unexpected, but a recent study demonstrated that NGF treatment promoted trkA translocation to the nucleus of PC12 cells (Moughal et al., 2004). Indeed, following internalization, numerous membrane-bound receptors translocated to the nucleus and elicited a biological response following agonist administration (Jans and Hassan, 1998; Reilley and Maher, 2001). With regard to NGF, the internalized trkA receptor promoted neuronal differentiation (Zhang et al., 2000). In addition, the neurotrophic factor BDNF was also identified in both neural cells and scar myofibroblasts, and may in concert with NGF promote neuronal differentiation and survival (Fahnestock, 1991; Gunn-Moore and Tavaré, 1998; Hee Han and Holtzman, 2000). The neural cell implicated in the synthesis of the neurotrophic factors was not determined, albeit previous studies have demonstrated that both glial cells and neurons synthesized NGF and BDNF (Fahnestock, 1991; Hee Han and Holtzman, 2000). Lastly, the biological role of neurotrophins in the scar may not be limited to neuronal differentiation and fiber formation. NGF may be directly involved in scar formation via the induction of the myofibroblast phenotype, and concomitant with BDNF induced angiogenesis (Donovan et al., 2000; Micera et al., 2001; Emanueli et al., 2002).

In summary, the present study has demonstrated that the scar region of the damaged rat heart contained reactive astrocytes, oligodendrocytes, and peripherin/neurofilament-positive neuronal cells and innervating fibers. In particular, the in vitro data indirectly supported the premise that reactive astrocytes, neurons, and possibly oligodendrocytes were derived from nestin-expressing neural stem cells. Neuronal cell differentiation and scar innervation may have occurred at least in part via the synthesis and secretion of NGF and BDNF by scar myofibroblasts and neural cells. Unexpectedly, both GFAP and neurofilament-M staining were detected in scar myofibroblasts. However, consistent with these latter observations, a recent study demonstrated that myofibroblasts located in the fibrotic liver of both humans and rats expressed GFAP and the neurotrophic factors NGF and BDNF (Cassiman et al., 2002). Additional studies are required to elucidate the physiological and/or pathophysiological role of neurons (including neuronal innervation) and glial cells in scar formation and remodelling post-MI.

ACKNOWLEDGMENTS

A. Calderone is a "Chercheur-Senior du Fonds de la recherche en santé du Québec" and Louis-Eric Trudeau is a "Chercheur-Junior II du Fonds de la recherche en santé du Québec."

LITERATURE CITED

Almazan G, Vela JM, Molina-Holgado E, Guaza C. 2001. Re-evaluation of nestin as a marker of oligodendrocyte lineage cells. Microsc Res Tech 52:753–765.

Cassiman D, Libbrecht L, Desmet V, Denef C, Roskams T. 2002. Hepatic stellate cell/myofibroblast subpopulations in fibrotic human and rat livers. J Hepatol 36:200–209.

Colombo F, Gosselin H, El-Helou V, Calderone A. 2003. β-adrenergic receptor-mediated DNA synthesis in cardiac fibroblasts proceeds via a phosphatidylinositol 3-kinase dependent pathway refractory to the antiproliferative action of cyclic AMP. J Cell Physiol 195:322–330.

Delsite R, Djakiew D. 1999. Characterization of nerve growth factor precursor protein expression by human prostate stromal cells: A role in selective neurotrophin stimulation of prostate epithelial cell growth. Prostate 41:39–48.

Donovan MJ, Lin MI, Wiegn P, Ringstedt T, Kraemer R, Hahn R, Wang S, Ibanez CF, Rafii S, Hempstead BL. 2000. Brain derive neurotrophic factor is an endothelial survival factor required for intramyocardial vessel stabilization. Development 127:4531–4540.

Edwards RH, Selby MJ, Gracia PD, Rutter WJ. 1988. Processing of the native nerve growth factor precursor to form biologically active nerve growth factor. J Biol Chem 263:6810–6815.

Emanueli C, Salis MB, Pinna A, Graiani G, Manni L, Madeddu P. 2002. Nerve growth factor promotes angiogenesis and arteriogenesis in ischemic hindlimbs. Circulation 106:2257–2262.

Fahnestock M. 1991. Structure and biosynthesis of nerve growth factor. Curr Top Microbiol Immunol 165:1–26.

Gabbiani G. 1998. Evolution and clinical implications of the myofibroblast concept. Cardiovasc Res 38:545–548.

Gunn-Moore FJ, Tavaré JM. 1998. Progress toward understanding the molecular mechanisms of neurotrophic factor signalling. Cell Signal 10:151–157.

Hao HN, Zhao J, Thomas RL, Parker GC, Lyman WD. 2003. Fetal human hematopoietic stem cells can differentiate sequentially into neural stem cells and then astrocytes in vitro. J Hematother Stem Cell Res 12:23–32.

Hasan W, Zhang R, Liu M, Warn JD, Smith PG. 2000. Coordinate expression of NGF and α-smooth muscle actin mRNA and protein in cutaneous wound tissue of developing and adult rats. Cell Tissue Res 300:97–109.

Hee Han B, Holtzman DM. 2000. BDNF protects the neonatal brain of hypoxic-ischemic injury *in vivo* via the ERK pathway. J Neurosci 20:5775–5781.

Jans DA, Hassan G. 1998. Nuclear targeting by growth factors, cytokines and their receptors: A role in signalling? Bioessays 20:400–411.

Johansson CB, Momma S, Clarke DL, Risling M, Lendahl U, Frisen J. 1999. Identification of a neural stem cell in the adult mammalian central nervous system. Cell 96:25–34.

Lendahl U, Zimmerman LB, McKay RD. 1990. CNS stem cells express a new class of intermediate filament protein. Cell 60:585–595.

Lin RC, Matesic DF, Marvin M, McKay RD, Brustle O. 1995. Re-expression of the intermediate nestin in reactive astrocytes. Neurobiol Dis 2:79–85.

Liu M, Warn JD, Fan Q, Smith PG. 1999. Relationships between nerves and myofibroblasts during cutaneous wound healing in the developing rat. Cell Tissue Res 297:423–433.

Matsuda H, Koyama H, Sato H, Sawada J, Itakura A, Tanaka A, Matsumoto M, Konno K, Ushio H, Matsuda K. 1998. Role of nerve growth factor in cutaneous wound healing: Accelerating effect in normal and healing impaired diabetic mice. J Exp Med 187:297–306.

Menet V, Gimenez Y, Ribotta M, Chauvet N, Drian MJ, Lannoy J, Colucci-Guyon E, Privat A. 2001. Inactivation of glial fibrillary acidic protein gene, but not that of vimentin, improves neuronal survival and neurite growth by modifying adhesion molecule expression. J Neurosci 21:6147–6158.

Micera A, Vigneti E, Pickholtz D, Reich R, Pappo O, Bonini S, Maquart FX, Aloe L, Levi-Schaffer F. 2001. Nerve growth factor displays stimulatory effects on skin and lung fibroblasts, demonstrating a direct role in tissue repair. PNAS 98:6162–6167.

Moughal NA, Waters C, Sambi B, Pyne S, Pyne NJ. 2004. Nerve growth factor signalling involves interaction between the TrkA receptor and the lysophosphatidate receptor 1 systems: Nuclear translocation of the lysophosphatidate receptor 1 and TrkA receptors in pheochromocytoma 12 cells. Cell Signal 16:127–136.

Nguyen QT, Colombo F, Clement R, Rouleau JL, Calderone A. 2003. AT_1 receptor antagonist therapy preferentially ameliorated right ventricular function and phenotype during the early phase of remodeling post-MI. Br J Pharmacol 138:1485–1494.

Oh H, Bradfute SB, Gallardo TD, Nakamura T, Gaussin V, Mishina Y, Pocius J, Michael LH, Behringer RR, Garry DJ, Entman ML, Schneider MD. 2003. Cardiac progenitor cells from adult myocardium: Homing, differentiation and fusion, after infarction. PNAS 100:12313–12318.

Orlic D, Kajstura J, Chimenti S, Jakoniuk I, Anderson SM, Li B, Pickel J, McKay R, Nadal-Ginard B, Bodine DM, Leri A, Anversa P. 2001. Bone marrow cells regenerate infarcted myocardium. Nature 410:701–705.

Reilley JF, Maher PA. 2001. Importin β-mediated nuclear import of fibroblast growth factor receptor: Role in cell proliferation. J Cell Biol 152:1307–1312.

Rice AC, Khaldi A, Harvey HB, Salman NJ, White F, Fillmore H, Bullock MR. 2003. Proliferation and neuronal differentiation of mitotically active cells following traumatic brain injury. Exp Neurol 183:406–417.

Rogister B, Ben-Hur T, Dubois-Dalcq M. 1999. From neural stem cells to myelinating oligodendrocytes. Mol Cell Neurosci 14:287–300.

Sanchez-Ramos J, Song S, Cardozo-Pelaez F, Hazzi C, Stedeford T, Willing A, Freeman TB, Saporta S, Janssen W, Patel N, Cooper DR, Sanberg PR. 2000. Adult bone marrow stromal cells differentiate into neural cells in vitro. Exp Neurol 164:247–256.

St Gelais F, Legault M, Bourque MJ, Rompre PP, Trudeau LE. 2004. Role of calcium in neurotensin-evoked enhancement in firing in mesencephalic dopamine neurons. J Neurosci 24:2566–2574.

Sun Y, Weber KT. 2000. Infarct scar: A dynamic tissue. Cardiovasc Res 46:250–256.

Toma JG, Akhavan M, Fernandes KJ, Barnabe-Heider F, Sadikot A, Kaplan DR, Miller FD. 2001. Isolation of multipotent adult stem cells from the dermis of mammalian skin. Nat Cell Biol 3:778–784.

Vracko R, Thorning D, Frederickson RG. 1990. Fate of nerve fibers in necrotic, healing and healed rat myocardium. Lab Invest 63:490–501.

Zhang Y, Moheban BR, Conway A, Bhattacharyya A, Segal RA. 2000. Cell surface Trk receptors mediate NGF-induced survival while internalized receptors regulate NGF-induced differentiation. J Neurosci 20:5671–5678.

Zhou S, Chen LS, Miyauchi Y, Miyauchi M, Kar S, Kangavari S, Fishbein MC, Sharifi B, Chen PS. 2004. Mechanisms of cardiac nerve fiber sprouting after myocardial infarction in dogs. Circ Res 95:76–83.